2.3 Micro-pattern detector facility at MIT-BATES

2.3.1 Introduction

2.3.2 GEM tracking detector concept

2.3.3 R&D results and micro-pattern detector utilization

2.3.3.1 Overview of R&D activities

2.3.3.2 COMPASS experience with a triple-GEM detector

2.3.4 Future GEM tracking application

2.3.4.1 STAR

2.3.4.2 eRHIC

2.3.4.3 Linear collider

2.3.5 Layout of a micro-pattern facility at MIT-BATES

2.3.5.1 Requirements

2.3.5.2 Layout

2.3.5.3 Equipment

2.3.5.4 Manpower

2.3.5.5 Cost

2.3.6 Summary

2.3 Micro-pattern detector facility at MIT-BATES

2.3.1 Introduction (ok)

Gaseous detectors in particular multi-wire proportional chambers (MWPC) introduced by Georges Charpak in 1968 at CERN [1] have a long tradition and are widely used in nuclear and particle physics as position-sensitive devices. Other areas of their successful application include astrophysics, medical diagnostics and biology [2]. The invention of the MWPC has been awarded by the Nobel Prize of Physics in 1992.

After its first introduction, the MWPC concept has been applied and extended in various detector variants such as drift chambers, time projection chambers and time expansion chambers [3-6]. Despite continued improvements in their performance characteristics, granularity and rate capabilities turned out to be limiting factors in particular for high luminosity applications in nuclear and particle physics.

In order to overcome those performance limits, a "second generation of gaseous detectors" was introduced which promised to be superior in terms granularity and rate performance. The micro-strip gas chamber (MSGC) was first described by A. Oed in 1988 [7]. It consists of tiny metal strips over a thin glass substrate which form an alternate structure of anode and cathode strips. The basic underlying principle is similar to that in case of a multi-wire proportional chamber. However, the application of photolithographic techniques allowed to manufacture rather fine structures which resulted in a substantial improvement in granularity. Furthermore, the space charge build up, which is one limiting factor for multi-wire proportional chambers in a high rate environment, is reduced due to the ability for fast positive ion collection. This provides a higher rate capability. This "second generation of gaseous generators" is usually referred to as "micro-pattern detectors". A review of their development and application can be found in [8].

Despite those promising features, their long-term and high-rate performance revealed several weaknesses. Under sustained radiation, polymerization processes lead to the deposition of an insulating layer on the metal anode and cathode strips and thus degraded the performance. Discharge effects due to large energy losses for example by heavy ionizing particles have shown to potentially lead permanent damage of the metal strips.

In order to overcome those limitations, several solutions have been suggested some of which are by now employed in several running experiments in nuclear and particle physics. The "Compteur à Trous" (CAT) is based on avalanche multiplication in narrow holes [9]. The MICROMEGAS concept uses a narrow gas parallel plate multiplication [10]. The Gas-Electron Multiplier (GEM) idea exploits a thin insulation foil, metal-clad on both sides which is perforated by a regular dense hole pattern [11].

It is in particular the application of the GEM-type tracking detectors which promises to have a wide-spread usage at future high-luminosity nuclear and particle physics experiments. The COMPASS experiment is successfully operating 20 triple GEM

detectors [12]. Those detectors have been design and constructed at CERN, in particular the manufacturing of the GEM foils. An outstanding issue in the application of GEM-type tracking detectors is the commercial manufacturing of GEM foils. Several academic institutions are actively involved in establishing such a process.

Micro-fabrication techniques, new materials and manufacturing methods recently developed in the field of Micro-Electro Mechanical Systems (MEMS) is presently experiencing an enormous boost. The application of MEMS technology in the design of novel gas detectors promises to establish a "third generation of gaseous detectors" [13].

Several groups within the Division of Nuclear and Particle Science of the Department of Physics at MIT are strongly considering GEM-type tracking detectors at future experiments such as for the STAR tracking upgrade and the NLC and eRHIC tracking system. Such an effort will require a clean room laboratory to handle and inspect for example GEM-foils besides the actual detector assembly. This has led to the following proposal of a dedicated micro-pattern facility at MIT-BATES laboratory. This is a unique opportunity within the US nuclear and particle physics field since such a facility has so far been concentrated outside the US. It will at the same time provide a facility to conduct R&D work on the development of novel "third generation gaseous detectors". Such novel detector concepts promise to have various applications outside the field of nuclear and particle physics.

The proposal starts with a brief overview of the GEM tracking detector concept followed by an overview of current R&D activities and future applications. The layout including a cost estimate for the clean-room setup and personnel is presented at the end.

References: (ok)

[1] G. Charpak et al., *Nucl. Instr. and Meth*. **62** (1968) 262.
[2] F. Sauli, *Nucl. Instr. and Meth.* **A419** (1992) 1; *Nucl. Instr. and Meth.* **A323** (1992) 1.
[3] F. Sauli, "New developments in gaseous detectors" in "Techniques and concepts of high-energy physics", T. Ferbel, Editor (Plenum 1983) 301.
[4] G. Charpak and F. Sauli, Ann. Rev. Nucl. Part. Sci. (1984) 285.
[5] W. Blum and G. Rolandi, "Particle detection with drift chambers", Springer-Verlag, Berlin, 1993.
[6] C. Grupen, "Particle Detectors", University Press, Cambridge, 1996.
[7] A. Oed, *Nucl. Instr. and Meth.* **A263** (1988) 351.
[8] F. Sauli and A. Sharma, *Ann. Rev. Nucl. Part. Sci.* **49** (1999) 341.
[9] F. Bartol et al., *J. Phys. III France* **6** (1996) 337.
[10] I. Giomataris et al., Nucl. Instr. and Meth. A376 (1996) 29.
[11] F. Sauli, *Nucl. Instr. and Meth.* **A386** (1997) 531.
[12] C. Altunbas et al., *Nucl. Instr. and Meth.* **A490** (2002) 177.
[13] O. Bouianov, private communications.

2.3.2 Micro-pattern tracking detector concept

Several new concepts of novel gas ionization detectors, referred to as "second generation of gaseous detectors" in the introduction of this proposal, have been presented. An overview can be found in [1-3].

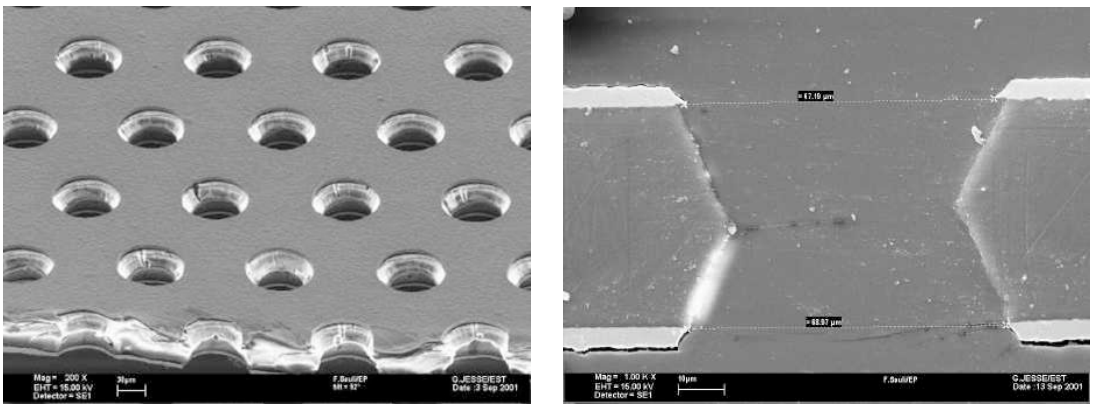

Figure 3: *Electron microscope picture of a GEM foil (left) and cross-section view through one hole (right).*

Two types of micro-pattern additions to overcome the limitations of micro-strip gas chambers (MSGC) have been extensively studied. Those are the Gas Electron Multiplier (GEM) [4] and MICROMEGAS [5].
A GEM is made by a thin (50μm) Kapton foil which are metalized from both sides by a ~5μm layer of copper each with a large number of microscopic holes of ~70μm at a pitch of ~140μm. An electron microscope picture of a GEM foil is shown in Figure 3 (left). A detailed cross-section view is shown Figure 3 (right) which clearly shows a double-conical shape as a consequence of the chemical etching process. The GEM manufacturing technique was developed by the CERN-EST-DEM workshop. The process starts with the production of two identical masks whose pattern is transferred to the foils which are coated by a photo-sensitive layer by means of conventional printed-circuit board technology exposing the coated layers to UV light. Upon inserting the GEM foil in a gas filled volume between a drift cathode and a read-out anode and application of a voltage between the two sides (~300-500V), electrons released in the upper gas volume drift into holes, multiply (E~100 kV/cm) and transfer to the other side where they can be collected or further amplified. Ions which are created in the holes are quickly removed. The induced signal is thus completely dominated by electron collection and provides therefore fast timing characteristics which allows its usage in a high-radiation environment. A unique feature of this device is that the multiplication stage is electrically separated from the readout plane. This offers a wide freedom in the choice of the readout pattern, which can be realized using strips or pads all at ground potential. Gas amplifications can be obtained up to 10^6 in a wide range of operating gases and conditions, including strong magnetic fields [6,7]. Several GEM foils can be cascaded that allows to reach a higher gas amplification and the same time avoids the problem with

discharges in a presence of heavily ionizing particles. The COMPASS experiment is successfully operating 20 triple-GEM detectors. This will be discussed in more detail in section 2.4.

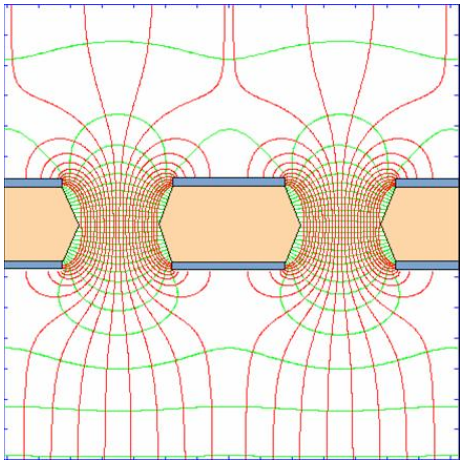

Figure 4: *Simulated field configuration inside a GEM hole [].*

A detailed description of Micromegas detectors can be found in [5, 8, 9]. It is a two-stage parallel plate electrode gas detector, where a low-field, 3.2mm thick conversion/drift space is separated from a 100μm thick amplification gap (E~30-50kV/cm) by a thin metal micromesh-type grid. Electrons which are created in the conversion gap initiate an avalanche and are collected by the readout structure whereas positive ions are removed by the grid. This gives rise to a rather fast timing response and thus its application in a high-rate radiation environment. The drift grid and the micromesh are made of 4μm thick Ni or Cu grids with 200-500 lines per inch. The needed parallelism between the micromesh grid and the anode is maintained by cylindrical spacers of 100-150μm diameter, and placed every ~2 mm. Those are printed on a thin substrate together with a readout structure by conventional lithography of a photo-resistive polyamide film. The thickness of the film defines the amplification gap. This is a cost effective and simple process that allows the construction of large detectors with good uniformity and energy resolution over the whole surface. Micromegas detectors are more sensitive to discharge problems compared to GEM detectors. The position resolution has been measured to be at the level of 12μm [11]. A timing resolution of 4.5ns has been presented in [10].

Both variants, Micromegas and GEM, represent a rather cost effective solution compared to silicon-based position sensitive detectors when space resolution for tracking detectors in the range of 30μm to few mm is required operating in a high-rate radiation environment.

2.3.3 R&D results and micro-pattern detector utilization

2.3.3.1 Overview of R&D activities

Micro-pattern detectors have been extensively studied in recent years and are currently used as tracking devices in high rate experiments. Current R&D activities are concentrated to optimize structure and operating parameters both for tracking detectors and TPC readout systems.

The main arguments to employ GEM and MicroMeGas type tracking detectors are as follows:

- Fast and "narrow" signal, dominated by electron collection with negligible "ion tail"
- Ion feedback suppression
- High precision in position reconstruction
- Staged amplification setups (Double and triple-type GEM detectors)
- Operation with different gases inside strong magnetic fields
- Simple "mechanical" construction, without the need for wire tensioning
- Small thickness and low material budget
- Flexible foil and read-out geometry
- Low distortions due to E X B (in amplification region)
- Applications in combination with other detector system (TPC, RHIC)

The most impressive example of micro-pattern detector utilization is the COMPASS experiment at CERN [12]. A system of 20 large size triple-GEM detectors and 6 MicroMeGas detectors have been built as part of the high-rate tracking system at COMPASS. Each GEM based chamber has an active area of 31x31cm^2. Each chamber provides a two-dimensional projective strip read-out at a pitch of 400μm. Good time (~15ns) and space (~47μm) resolution have been achieved. A cluster charge correlation between two orthogonal read-out strip projections offers a powerful tool for multi-track reconstruction. During the last two years, none of the readout channels were lost. The detector performance is stable since then. A detailed description on the construction and performance of the COMPASS GEM detector system will be discussed in the next section.
The MicroMeGas detectors built for the COMPASS experiment have a 40 x 40 cm^2 active area and are operated in a gas mixture of Ne-C_2H_6-CF_4 (80-10-10) with 360-420μm pitch strip read-out. A discharge rate of less than 0.1/spill was observed in the high-intensity muon beam of COMPASS. A time resolution of ~10 ns has been reached.

Several R&D activities are concentrated to study different variants for TPC readout systems on the basis of micro-pattern approaches [13, 14, 15] which are very promissing. GEM foils have been used in a combination with photo-converters to demonstrate a possibility to construct a "gas photo-tube" [16,17]. The GEM application with a

“reflective” CsI covering on a top of the “first” GEM foil can be used as a large size detector with high efficiency both to UV-photons and MIPs [15].

One of the most urgent needs is to find a company or laboratory to establish a GEM foil mass-production. So far, high-quality GEM foils have been only produced at CERN. Besides that, the setup of a micro-pattern facility is urgently needed to advance on detector R&D construction, in particular in the US. This provides a unique opportunity for MIT-BATES laboratory where several research groups at MIT are actively pursuing the application of GME-type tracking detectors in future nuclear and particle physics experiments. An overview of those activities will be given in the following part of this section.

References:

[1] F.Sauli NIM A419 (98) 189; NIM A461 (01) 47
[2] IEEE Nuclear Science Symposium, Micropattern Detectora Workshop, Nov 03.
[3] F.Sauli NIM A505 (03) 195
[4] F.Sauli NIM A386 (97) 531
[5] Y.Giomataris, Ph Rebourgeard, J.P.Robert, G.Charpak NIM A376 (96) 29
[6] R.Bouclier, et al. NIM A396 (97) 50; A.Bressan, et al. NIM A429 (99) 254;
G.Bencivenni et al. LHCb preprint (02), "A triple-GEM detector
with pad readout for high rate charged particle triggering".
[7] S.Roth, et al. RWTH Aachen, IEEE Nuclear Science Symposium, Nov 03,
"Study of GEM Structures for a TPC Readout"
[8] G.Charpak et al. NIM A412 (98) 47
[9] G.Barrouch et al. NIM A423 (99) 32
[10] J.Derre et al. NIM A449 (00) 314
[11] J.Derre et al. NIM A459 (01) 523
[12] C.Altunbas et al. CERN-EP/2002-008; B.Ketzer NIM A494 (02) 142
[13] M.T.Ronan, LBNL, IEEE Nuclear Science Symposium, Nov 03,
"Status of R&D Efforts for a Linear Collider TPC with Micropattern
Detector Readout"
[14] S.Kapler et al., Karlsruhe University, CERN;
IEEE Nuclear Science Symposium, Nov 03,
"Design and Construction of a GEM-TPC Prototype for R&D Purposes"
[15] D.Karlen, University of Victoria & TRIUMF, Berkeley LC-TPC meeting,
Oct, 03; "LC-TPC R&D Overview".
[16] D.Mormann et al. NIM A504 (03) 93
[17] A.Breskin et al. NIM A513 (03) 250

2.3.3.2 COMPASS experience with a triple-GEM detector

Introduction

The COMPASS (COmmon Muon and Proton Apparatus for Structure and Spectroscopy) experiment at CERN is a new fixed target experiment which is in operation since 2001. It is designed to explore the nucleon spin structure and spectroscopy of hadrons. The first goal of the experiment is to explore the gluon contribution to the nucleon using open charm production in the photon-gluon fusion process and the production of high p_T hadron pairs from deep inelastic scattering of polarized muons on polarized nucleons. In case of open charm production this requires the identification of D^0 and D^0 mesons from their decay products of $\pi^{\pm}$ and $K^{\pm}$ with momenta around 10GeV/c, and of D^* mesons, which decay into a D meson and a pion having a momentum of around 1.6GeV/c.

This program requires high intensity muon and hadron beams of $2*10^8$ muons of 160GeV per 5s spill, and 10^8 p, K and π per spill at 100-280GeV from the Super Proton Synchrotron (SPS). This sets stringent requirements on the high-rate and multi-track resolution capability. It requires fast, dead-time free readout electronics and low material budget to reduce multiple scattering.

The COMPASS experiment

A schematic layout of the COMPASS experiment is shown in Figure 1.

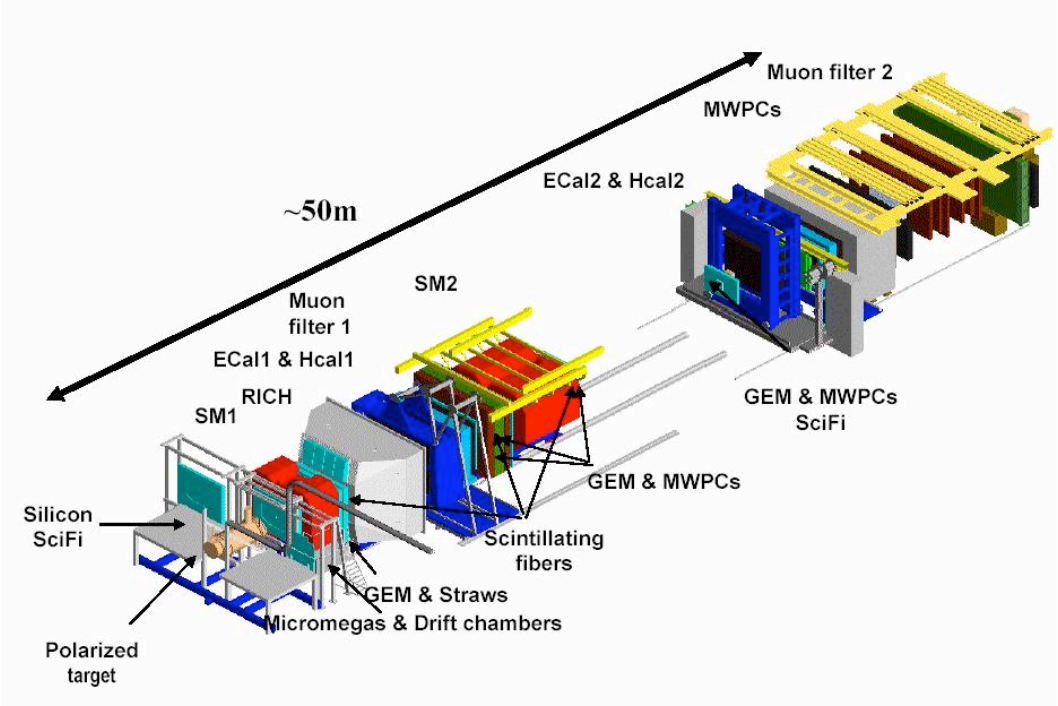

Figure 1: *Schematic layout of the COMPASS experiment.*

The experiment is laid out as a two-stage spectrometer. The first section covers an angular range of up to 220mrad in the vertical and 250mard in the horizontal plane It is located downstream of the target and includes the momentum analyzing magnet SM1 which is shown in Figure \ref{sec2_compass}. The second section which is located after the momentum analyzing magnet SM2 covers an angular range of up to 30mrad.

The tracking system is realized by various detector systems with increasing rate capability going closer to the beam axis where the particle flux is highest. The outermost tracking section is covered by the Large Area Tracker (LAT) which uses conventional Multi-wire Proportional Chambers together with several types of drift chambers.

The region between 2.5-3.0cm of radial distance from the beam region refers to the Very Small Area Tracking (VSAT) region and is laid out by a set of silicon micro-strip detectors and scintillating fiber detectors. The intermediate tracking region is covered by the Small Area Tracking (SAT) detector. It spans a radial distance of approximately 2.5cm to 40cm. Micro-pattern detection systems have been used for this tracking region. The area in front of the first momentum analyzing magnet (SM1) comprises three stations of Micromegas. Each station is made out of 4 planes with horizontal (X), vertical (Y) projections, and two projections inclined by ±45° (U,V). The area downstream of the first momentum analyzing magnet (SM1) is laid out by 10 GEM stations. Each GEM station is comprised by two GEM detectors which are rotated by 45° with respect to each other.

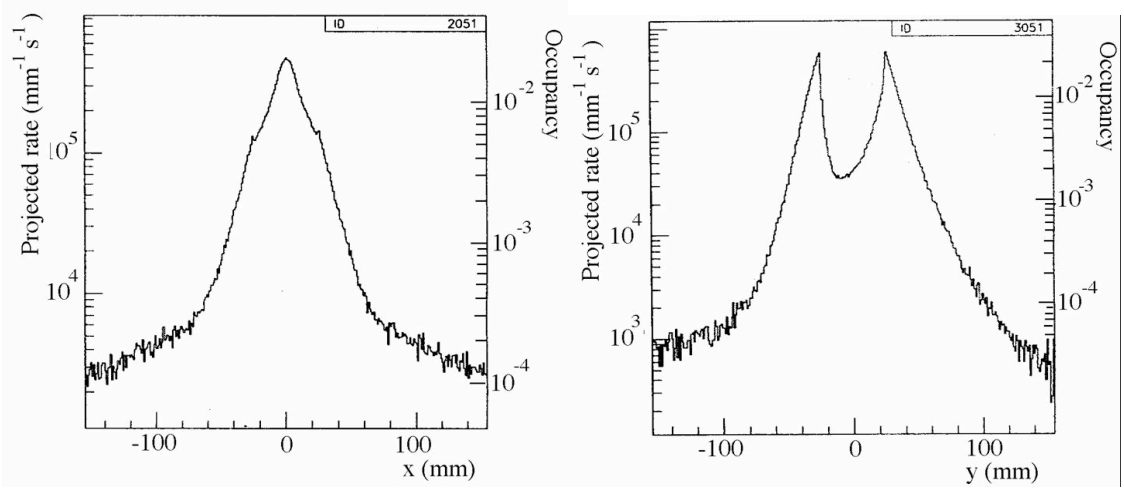

Figure 2: *Projected charged particle rates and occupancy as a function of the radial distance from the beam at GEM station 4 which is located \$15\,\$m downstream of the target \cite{sec2_compass_gem}.*

Figure 1 shows the projected charged particle rates and occupancy as a function of the radial distance from the beam at GEM station 4 which is located 15m downstream of the target. The average particle rate per strip for a GEM detector is expected to be around 30-40kHz with a maximum of up to 150kHz close to the beam axis. Those high rate requirements together with the demand for large area tracking capability, high spacial

resolution and low material budget has been realized with the installation of 20 large-size (31 X 31cm^2) GEM detectors.

The COMPASS triple-GEM tracking detector

a) Layout

The heart of the COMPASS GEM (Gas Electron Multiplier) \cite{sec2_sauli1} tracking detectors are 50μm thin Kapton foils which are metalized from both sides by a 5μm layer of copper each with a large number of microscopic holes of ~70μm diameter at a pitch of 140μm. An electron microscope picture of a GEM foil is shown in Figure 3 (left). A detailed cross-section view is shown in Figure 3 (right) which clearly shows a double-conical shape as a consequence of the chemical etching process.

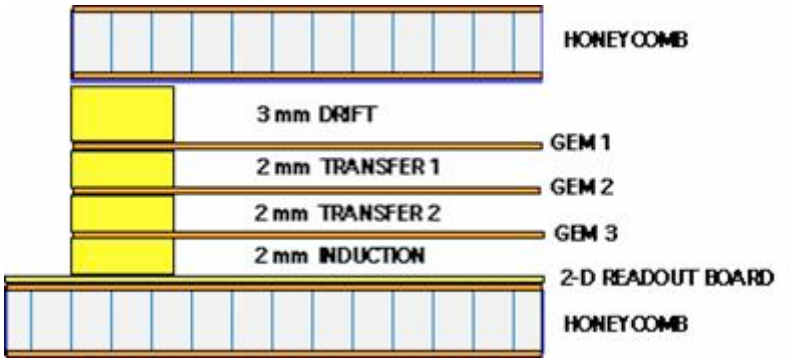

Figure 5: *Schematic cross-section view of the COMPASS triple GEM detector \cite{sec2_compass_gem}.*

Proportional gains of several thousand can be obtained in a wide range of operating gases and conditions \cite{sec2_bouclier}. The multiplication step and charge detection is performed on two separate electrodes which allows a large variety of readout structures which will be discussed in case of the COMPASS GEM detector in the following.

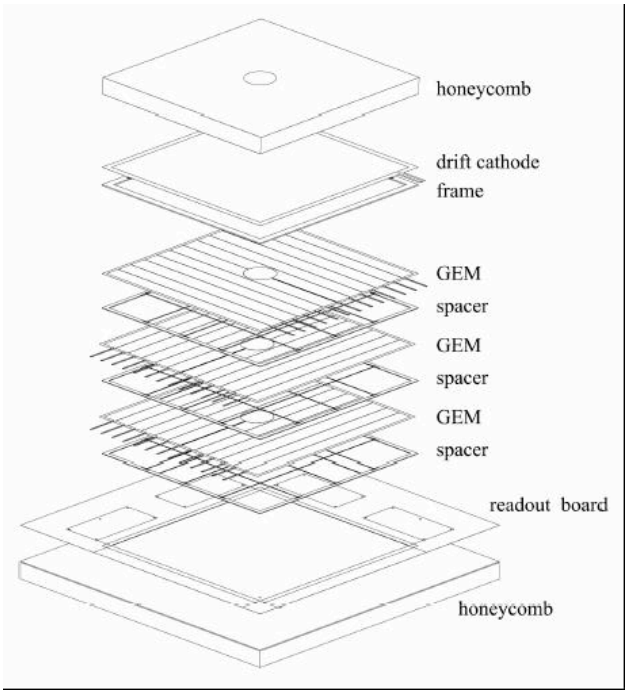

Figure 6: *Exploded view of the COMPASS triple GEM detector (left) and schematic cross-section view of the COMPASS triple GEM detector \cite{sec2_compass_gem}.}*

b) Assembly

An exploded view of the COMPASS triple GEM detector is shown in Figure \ref{sec2_gemdet1} together with a schematic cross-section view in Figure \ref{sec2_gemdet2}. A completed chamber is shown in Figure \ref{sec2_gemdet_pic}.

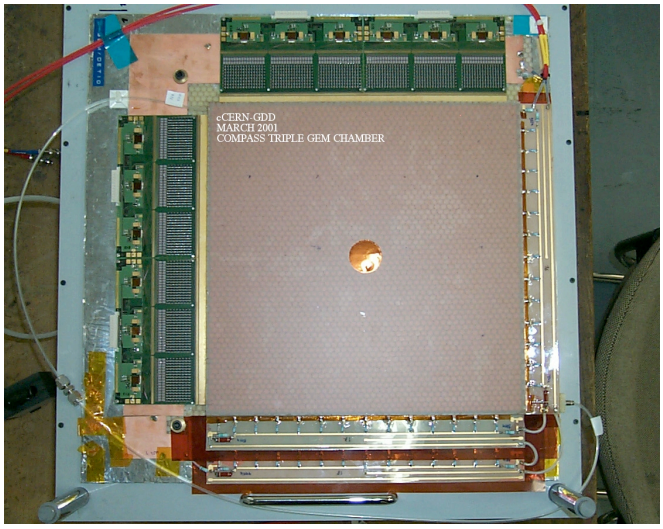

Figure 7: *Completed chamber including HV distribution and the two-dimensional readout electronics. The active area amounts to 31 X 31cm^2 \cite{sec2_compass_gem}.*

The top part is a honeycomb plate followed by the drift electrode, three GEM foils and the readout board which is attached to the lower honeycomb plate. The drift cell is 3mm thick whereas all other cell have a thickness of 2mm. Each cell is separated from each other by fiberglass strips which have a width of about 400μm which introduces only a small local efficiency loss. In order not to be swapped by the primary non-interacting beam, a central region of 50mm in diameter can be remotely disabled. In addition, each GEM foil is subdivided into 12 sectors which are separately connected externally to the voltage supply. This subdivision reduces the energy stored in each GEM foil. The charge which is released during a discharge is thus decreased and the probability that a discharge reaches the readout board which started between two GEM foils. A close-up view of a partitioned GEM foil is shown in Figure \ref{sec2_gemsec}.

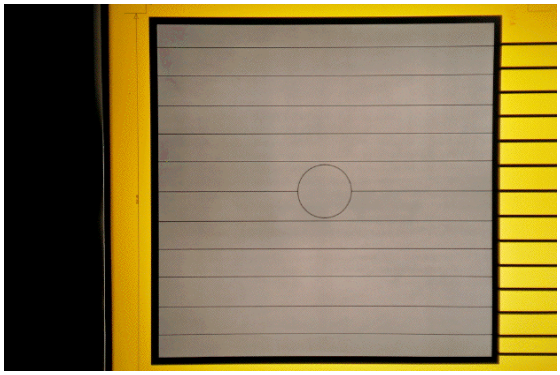

Figure 6: *Close-up view of a partitioned GEM foil which shows 12 rectangular sectors and one central 50mm diameter central sector \cite{sec2_compass_gem}.}*

The readout board is realized by a two-dimensional projective read-out of the signals which makes use of a printed circuit board with two layers of perpendicular copper strips at 400μm pitch which are separated by $50μm thick Kapton ridges. Each coordinate has 768 readout strips. This readout board has been manufactured using similar techniques of photo-lithographic methods as used for the fabrication of the GEM foils itself. A close-up view of the two-dimensional readout board can be seen in Figure \ref{sec2_readout}. An equal charge sharing between each readout layer is achieved by choosing the strip width of the top layer to be 80μm and 350μm for the bottom layer. The total active area amounts to 31 X 31cm^2.

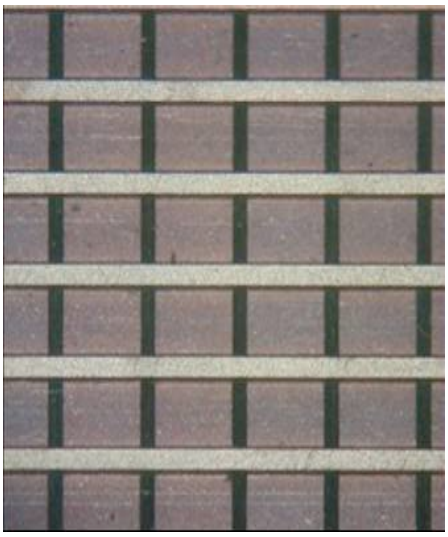

Figure 7: *Close-up view of the two-dimensional readout board \cite{sec2_compass_gem}.}*

c) Readout electronics

The readout electronics is based on the APV25 chip \cite{sec2_apv25} which is a 128-channel amplifier-shaper ASIC with an analogue pipeline of 192 cells for each input channel. This chip is based on the 0.25μm CMOS process which provides clear advantages in power consumption, noise performance and radiation tolerance. The amplified and shaped signals are sampled at a rate of 40MHz and stored in a pipeline with a latency of up to 160 clock cycles (4μs). Once a positive trigger decision has been issued, three consecutive samples of each channel are multiplexed and digitized by an ADC.

The APV25 chips has been developed for the CMS silicon tracker. It does not provide input protection from overload resulting from a discharge. An external circuit has been added for protection based on a pair of inverted high-speed signal diodes (BAV99) which are connected to ground, and a coupling capacitor 220pF to avoid leakage currents into the APV25 chip circuit.

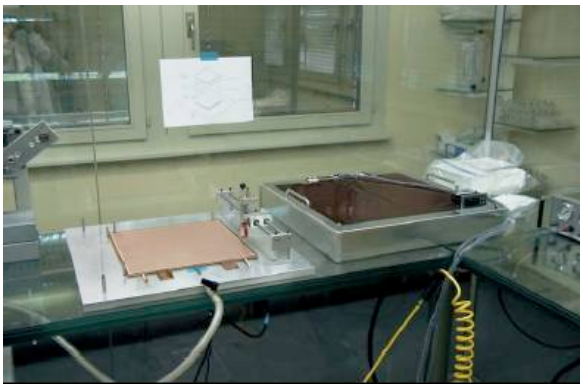

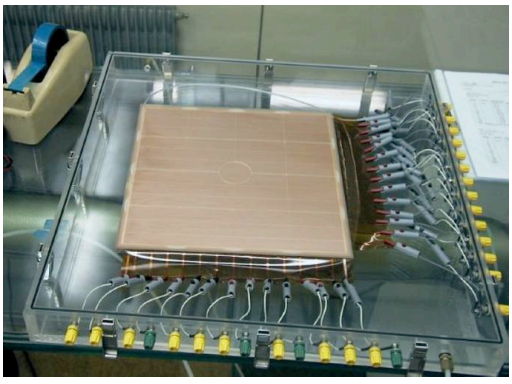

Figure 8: *Photograph of the mounting and gluing setup used for the COMPASS GEM detector construction (left). Photograph of the HV test-setup used to test the HV characteristics of each GEM foil prior to its actual installation \cite{sec2_gem_construction}.}*

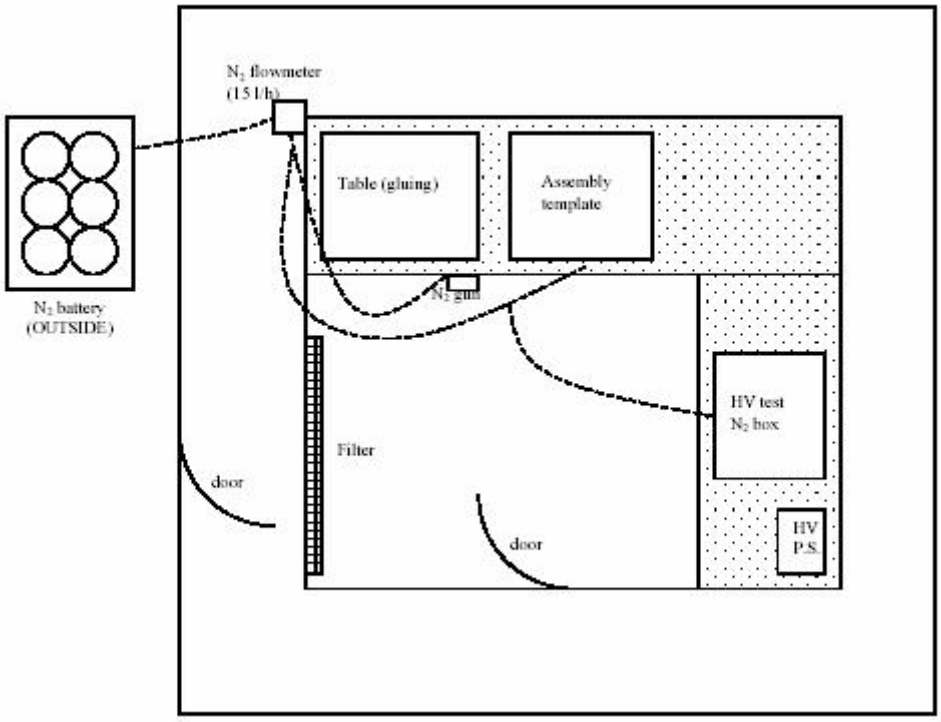

Figure 9: *Schematic layout of the COMPASS clean room setup \cite{sec2_gem_construction}.*

The assembly of the GEM detectors is entirely carried out in a clean room of at least class 1000 with temperature control and low moisture level (~40%). Protective clothing is always worn. A schematic overview of the clean room where the COMPASS GEM detectors are assembled is shown in Figure \ref{sec2_cleanroom}. Figure ref{sec2_mounting} (left) shows the mounting plate and gluing station used for the GEM detector construction. The HV test setup used for the GEM foils inside a nitrogen box is shown in Figure \ref{sec2_mounting} (right). The construction of the GEM detectors for the COMPASS experiment including a detailed description of the infrastructure, materials, procedure and quality requirements can be found in \cite{sec2_gem_construction}.

d) Performance

The following section provides a brief account of the main performance features of the COMPASS triple GEM detectors \cite{sec2_compass_gem}. Prior to the assembly of a GEM detector, each GEM foil is inspected and tested. First quality checks are performed before a foil leaves the GEM production facility such as a measurement of the resistivity

in air between the conductive GEM sides which has to exceed 2GΩ to be accepted. Once a GEM foil is accepted and ready to be taken to the actual GEM detector assembly facility which is carried in out in clean packing and left in clean storage units if necessary.

The HV characteristic is checked during the whole assembly operation, i.e. before mounting and during various assembly steps. This procedure is carried out in a nitrogen filled box which is shown in Figure \ref{sec2_mounting} (right). The box is flushed for several hours with nitrogen to decrease moisture followed by HV tests under continuous monitoring of the leakage current performance. A GEM foil is accepted if the leakage current is <5nA at 600V.

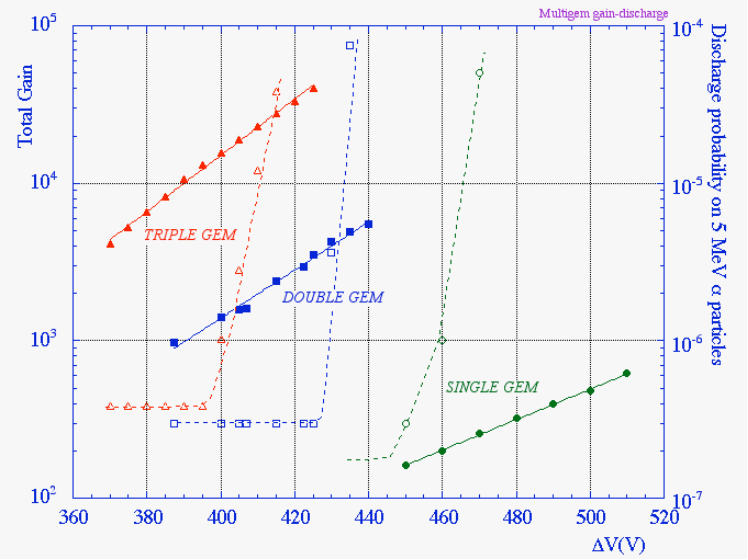

Figure 10: *Total gain as a function of the potential difference applied to each GEM foil for single, double and triple GEM detectors. Also shown is the discharge probability on exposure to a 6MeV α-particle, emitted by a ^{220}Rn source \cite{sec2_compass_gem}.}*

Figure \ref{sec2_gain} shows the total gain as a function of the potential difference applied to each GEM foil for single, double and triple GEM detectors. Also shown is the discharge probability on exposure to a 6MeV α-particle, emitted by a ^{220}Rn source. It is evident from these studies that a triple GEM detector can be safely operated over a wide operating range. The discharge probability is hardly measurable. Several foils thus allow sustaining large gains even in the presence of heavy ionizing particles.

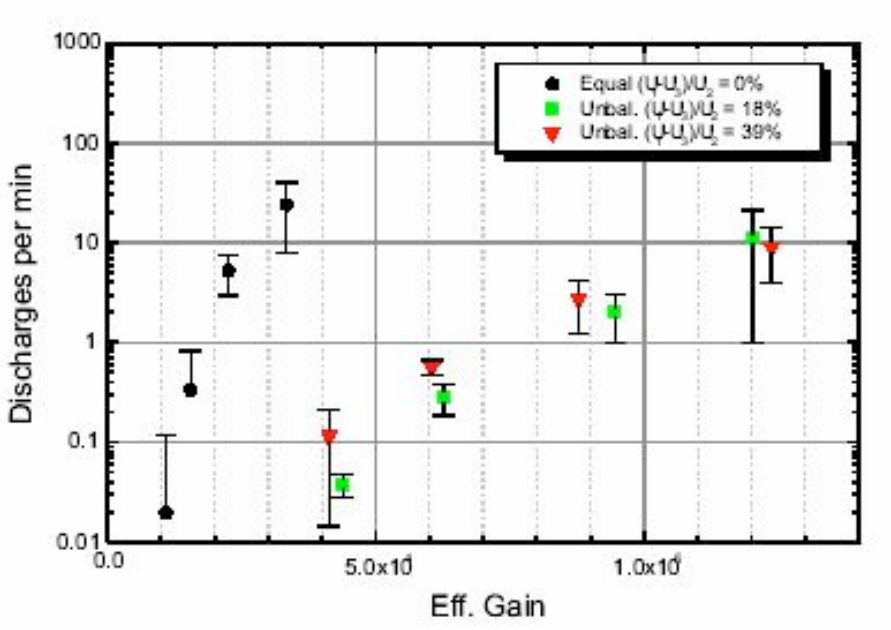

Figure 11: *Discharge rate as a function of the effective gain for different relative potential differences between the individual GEM foils \cite{sec2_gem_triple}.}*

It was found that the discharge probability under exposure to α-particles depends on the potential difference between the GEM foils \cite{sec2_gem_triple}. Figure \ref{sec2_rate_gem} shows the discharge rate as a function of the effective gain for different relative potential differences between the individual GEM foils. The discharge rate can be reduced if the first GEM foil is in fact operated at a higher gain compared to the third GEM foil.

It has been shown in \cite{sec2_gem_aging} that a 10 X 10cm^2 double GEM prototype detector is less sensitive to aging than other micro-pattern gas detectors. The COMPASS triple GEM detector was tested for aging effects by irradiating the detector using a beam of 8.9keV X-rays for about one month at rates of up to $2.5 \cdot 10^4$Hz/mm^2. No gain loss was observed even after collecting more than 7mC/mm^2 which corresponds to the total charge of seven years of operation in the radiation environment \cite{sec2_aging_discussion}.

Three triple GEM detector were tested in a test-beam experiment at the T11 beam-line of the CERN PS. The detectors were exposed for several weeks to a 3.6GeV charged particle beam of about 10^6 particles per 200ms spill. A set of scintillator counters was used to define a beam trigger. A silicon micro-strip detector provided an independent position measurement. Two of the three installed triple GEM detectors were equipped with the final readout electronics.

Figure \ref{sec2_pos_resolution} shows the difference of coordinate measurements between one triple GEM detector and the silicon micro-strip detector for both transverse coordinates. A Gaussian fit to these distributions yields a standard deviation of about\ 70μm. Taking into account the accuracy of the silicon micro-strip detector of

approximately 15µm and deteriorating effects from multiple scattering, this yields a position resolution of 40µm which agrees with previous prototype measurements \cite{sec2_position}.

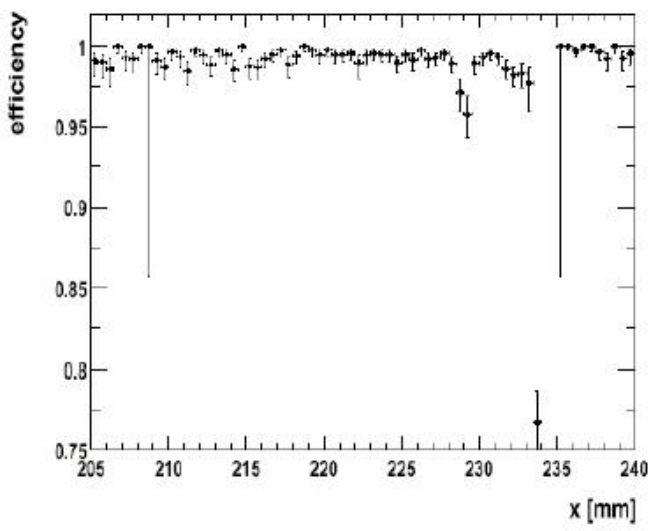

Figure 12: *Measured efficiency plotted as a function of the local position \cite{sec2_compass_gem}.}*

The silicon micro-strip detector has been also used as a reference for an efficiency measurement. The measured efficiency is plotted in Figure \ref{sec2_eff} as a function of the local position. Local losses are found which are due to spacers and sector boundaries. Efficiencies in access of 98% are achieved for the actual active area.

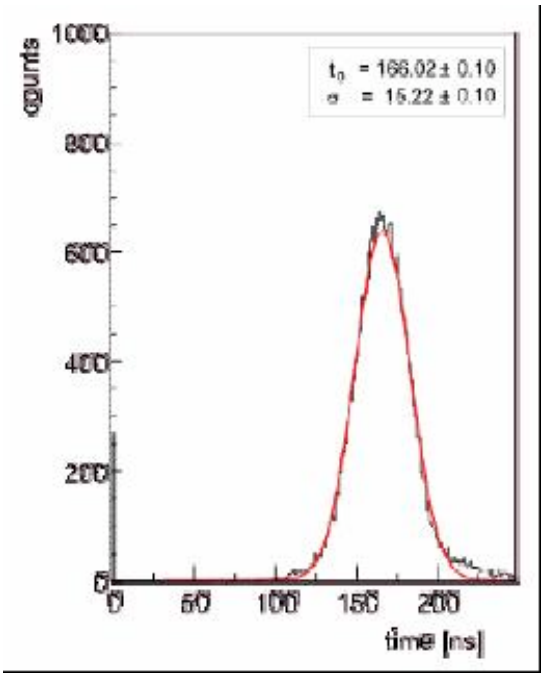

Figure 13: *Time resolution of the triple GEM detector which has been determined to be 15.2 ± 0.1ns during the CERN PS test-beam experiment \cite{sec2_compass_gem}.}*

Figure \ref{sec2_time} shows the time resolution of the triple GEM detector which has been determined to be 15.2 ± 0.1ns during the test-beam experiment. This value represents a convolution of physical and electronic effects compared to the intrinsic resolution of about 7ns rms \cite{sec2_position}.

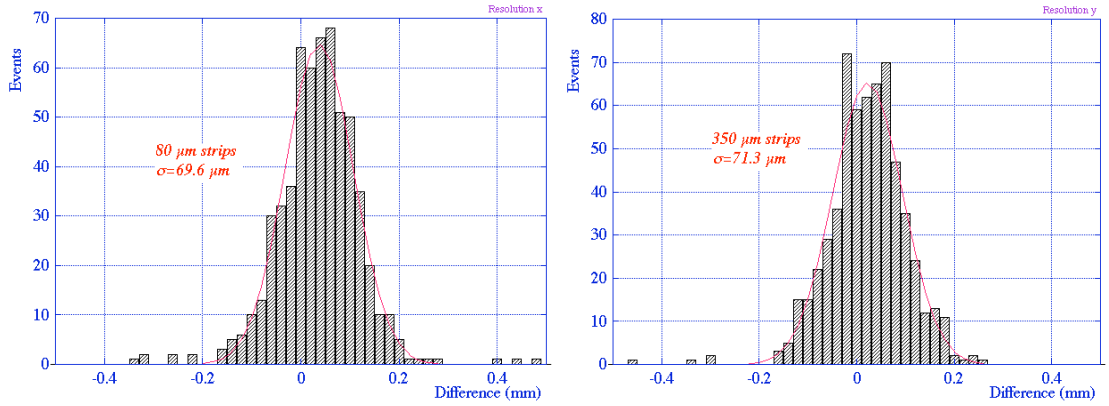

Figure 14: *Difference of coordinate measurements between one triple GEM detector and the silicon micro-strip detector for both transverse coordinates determined during the CERN PS test-beam experiment \cite{sec2_compass_gem}.*

A set of 20 triple GEM detector are in operation as a integral part of the COMPASS experiment. The performance of those novel new tracking devices so far have clearly shown that they meet the requirements for tracking devices in modern high-energy physics experiments in terms of their rate capabilities, timing characteristics, position resolution and tracking efficiency.

References

\bibitem{sec2_sauli1} F. Sauli, \NIMA 386 (1997) 531.
\bibitem{sec2_bouclier} R. Bouclier et al., \NIMA 396 (1997) 50.
\bibitem{sec2_gem_construction} M. Capeans et al., `Construction of GEM detectors for the
COMPASS experiment', CERN-EP/TA1, Technical note TA1/00-03
\bibitem{sec2_gem_aging}S. Bachmann et al., \IEEE 47 (2000) 1412.
\bibitem{sec2_gem_triple}B. Ketzer et al., \IEEE 49 (2002) 5.
\bibitem{sec2_position}A. Bressan et al. \NIMA 425 (1999) 262.
\bibitem{sec2_apv25}M.J. French et al., \NIMA 466 (2001) 359.
\bibitem{sec2_aging_discussion}C. Altunbas et al., `Aging measurements with gas electron multiplier (GEM)',
International Workshop on Aging Phenomena in Gaseous Detectors, Hamburg, Germany, October 2-5, 2003, CERN-EP-2001-091